

Dark solitons in erbium-doped fiber lasers based on indium tin oxide as saturable absorbers

Jia Guo ^a, Huanian Zhang ^{a, b, *}, Zhen Li ^a, Yingqiang Sheng ^a, Quanxin Guo ^a, Xile Han ^a, Yanjun Liu ^c, Baoyuan Man ^a, Tingyin Ning ^{a, b}, Shouzhen Jiang ^{a, b, **}

^a School of Physics and Electronics, Shandong Normal University, Jinan 250014, China

^b Shandong Provincial Key Laboratory of Optics and Photonic Device, Jinan 250014, China

^c Department of Electrical and Electronic Engineering, Southern University of Science and Technology, Shenzhen 518055, China



ARTICLE INFO

Article history:

Received 3 February 2018

Received in revised form

24 February 2018

Accepted 26 February 2018

Keywords:

Dark solitons

Indium tin oxide

Nonlinear absorption properties

Saturable absorber

Ultrafast photonics

ABSTRACT

Dark solitons, which have good stability, long transmission distance and strong anti-interference ability. By using a coprecipitation method, the high quality indium tin oxide (ITO) were prepared with an average diameter of 34.1 nm. We used a typical Z-scan scheme involving a balanced twin-detector measurement system to investigated nonlinear optical properties of the ITO nanoparticles. The saturation intensity and modulation depths are 13.21 MW/cm² and 0.48%, respectively. In an erbium-doped fiber (EDF) lasers, we using the ITO nanoparticles as saturable absorber (SA), and the formation of dark soliton is experimentally demonstrated. The generated dark solitons are centered at the wavelength of 1561.1 nm with a repetition rate of 22.06 MHz. Besides, the pulse width and pulse-to-pulse interval of the dark solitons is ~1.33ns and 45.11 ns, respectively. These results indicate that the ITO nanoparticles is a promising nanomaterial for ultrafast photonics.

© 2018 Elsevier B.V. All rights reserved.

1. Introduction

In nonlinear systems, solitons can be divided into bright and dark ones [1]. The formation of dark solitons is the same as that of bright solitons, which is an intrinsic feature of the nonlinear light propagation in the normal dispersion regimes [2,3]. Recently, dark solitons as a unique optical phenomenon are widely investigated in nonlinear and ultra-fast optics [4–10]. Compared with the bright solitons, dark solitons have many advantages, such as high stability, long transmission distance, small time jitter and strong anti-interference ability [11]. Thus, dark soliton pulses have wide application potential in the fields of precision measurement, all-optical nonlinear communication and nonlinear optics [12–16].

Dark solitons formed in the erbium-doped fiber (EDF) laser were obtained in Ref. [17] firstly, since then, researchers have explored different saturable absorbers (SAs) based on various nanomaterials for generating dark solitons in the EDF laser. For example, Wei et al.

demonstrated dark solitons with WS₂-based SAs in the EDF fiber laser [18]; Liu et al. observed dark solitons in EDF lasers based on Sb₂Te₃ saturable absorbers [19]; Zhao et al. indicated that the generation of L-band bright and dark pulses can be achieved within a graphene-oxide (GO) mode-locked EDF laser [20]. However, all of these 2D materials have an inefficient light-matter interaction. This becomes their bottleneck in the application of the optoelectronic devices [21]. Therefore, a new SAs with strong light-matter interaction, broad saturable absorption region, ultrafast recovery time and cost-effective fabrication for generation of dark solitons pulses is highly desirable and yet to be developed. By analyzing the recent developments on different SAs based on 2D semiconductors, graphene and zero-gap materials of semimetals and topological insulator, we can refer to the stable sequence below to select the SAs: oxide plasmonic nanocrystals > graphene, transition metal dichalcogenides (TMDs) > black phosphorus (BP) and other metal compounds (selenide, telluride, etc.) [22]. Oxide plasmonic nanocrystals will become promising nanomaterials because of their unique properties, such as efficient light-matter interaction, excellent optical nonlinearity, outstanding plasmonic absorption characteristic and mature preparation process [23,24]. So, using oxide plasmonic nanocrystals as SAs is the ideal choice for the formation of dark solitons.

* Corresponding author. School of Physics and Electronics, Shandong Normal University, Jinan 250014, China.

** Corresponding author. School of Physics and Electronics, Shandong Normal University, Jinan 250014, China.

E-mail addresses: zhn@sdu.edu.cn (H. Zhang), jiang_sz@126.com (S. Jiang).

In our work, indium tin oxide (ITO) as one of oxide plasmonic nanocrystals was employed for dark solitons. To our knowledge, this is the first demonstration that the ITO nanoparticles are used as SAs for dark solitons pulses generation. There are three reasons for using the ITO nanoparticles as SAs. First, the conductive oxides has a lower carrier density, so the plasmonic absorption of ITO in the near infrared region (NIR) has a strong peak and a broad bandwidth [25]. Second, the peak of the plasmonic absorption can be adjusted from 1600 to 2200 nm by changing the concentration of tin doped in ITO [26]. This characteristic endow the ITO an even broader saturable absorption region. Third, recent studies have showed that thin films of the ITO demonstrate large optical nonlinearity. Besides, they report that the ITO have a ultrafast recovery time of about 360 fs [24]. High quality ITO nanoparticles with an average diameter of 34.1 nm was prepared by using a coprecipitation

method. By directly dropping ITO colloidal liquid between two fiber connectors in EDF lasers, the dark soliton formation is experimentally demonstrated. A series of optical spectra of dark solitons pulses based the ITO SAs are presented. These results will make great significance for further studies of dark soliton. In addition, this study shows that the ITO is a promising candidate for the ultrafast photonics.

2. Experimental step

2.1. Preparation of ITO nanoparticles

Nanocrystalline ITO powders were obtained by using a coprecipitation method. First, by adding indium into the sulfuric acid, the $In_2(SO_4)_3$ solution was obtained. And then the $In_2(SO_4)_3$ solution

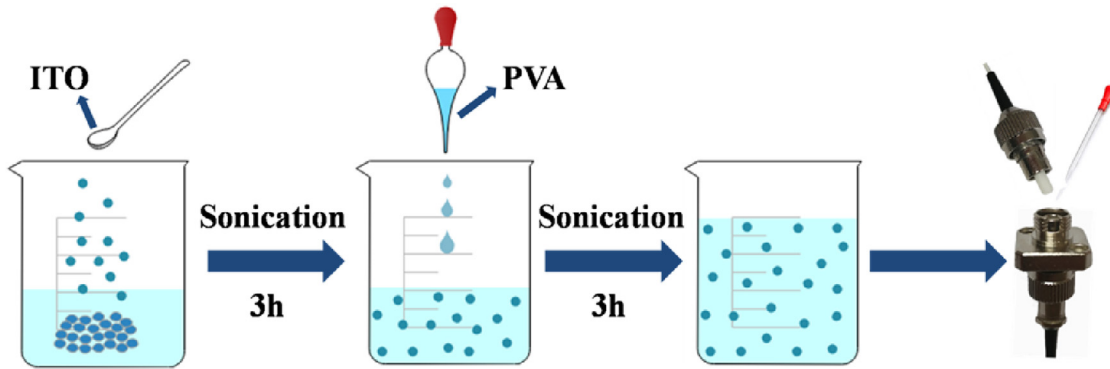


Fig. 1. Fabrication process of the ITO SAs.

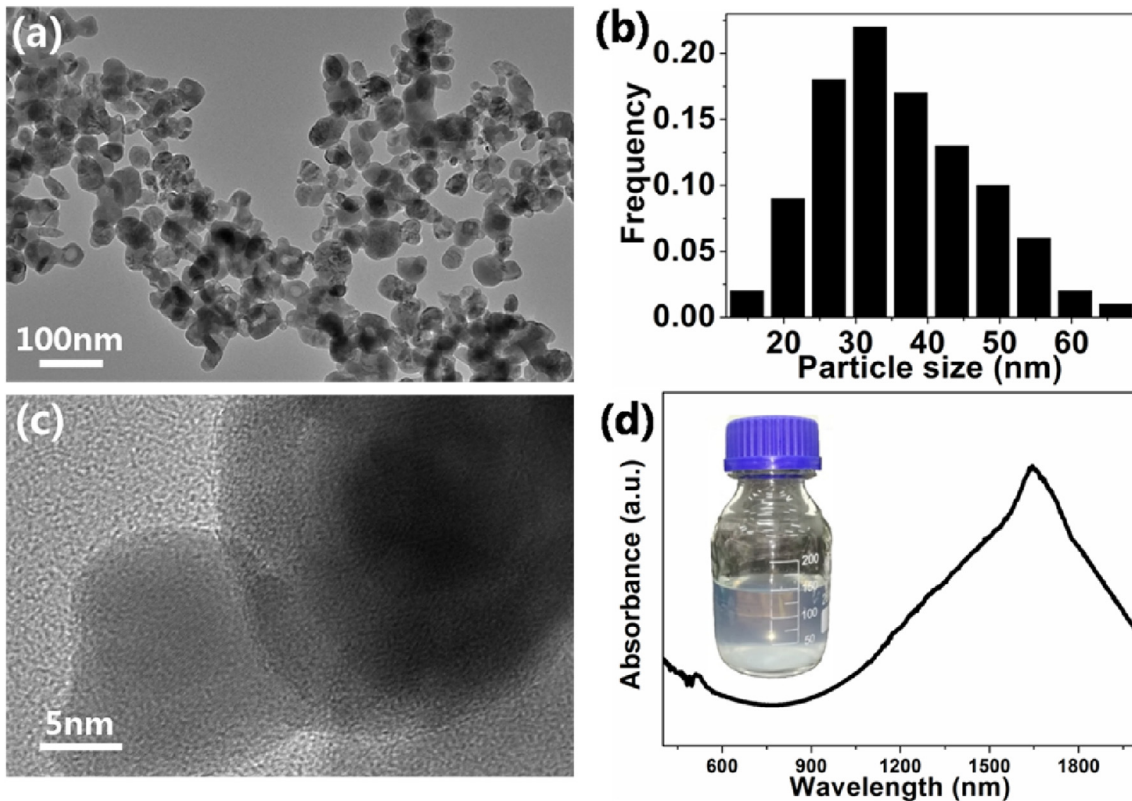


Fig. 2. (a) TEM image of the ITO nanoparticles. (b) The particle size distribution of the ITO nanoparticles from the TEM image. (c) HRTEM image of the ITO nanoparticles. (d) Absorption spectrum of the ITO dispersion solution.

and the SnCl_4 solution were mixed at $\text{In}_2\text{O}_3/\text{SnO}_2 = 9/1$ (mass ratio) and reacted at a constant temperature of 70°C . The pH value of the mixed solution is kept at 7 by adding 2 mol/L NaOH solution under high speed stirring. Continue stirring for 30 min so that the chemical reaction is complete. Finally, through a series of processes, such as filtration, washing, drying, calcination, and grinding, the coprecipitation precursor become ITO nanoparticles.

2.2. Fabrication of ITO SAs

The diagram of the fabrication of ITO SAs is shown in Fig. 1. First, in order to obtain the ITO dispersion solution, 0.012 g ITO

nanoparticles were added to 50 ml deionized water with ultrasonic treatment for 3 h. Second, the 100 ml of 10% polyvinyl alcohol (PVA) solution was added to the ITO dispersion solution. And the mixture was treated with ultrasonic for 3 h to get the ITO colloidal liquid. Finally, the ITO SAs was successfully prepared by directly dropping ITO colloidal liquid between two fiber connectors.

2.3. Apparatus and characterization

The transmission electron microscopy (TEM) image of the ITO nanoparticles was obtained by using a TEM system (Hitachi H-800). Ultraviolet-visible spectrophotometer (UV-vis Spectrophotometer,

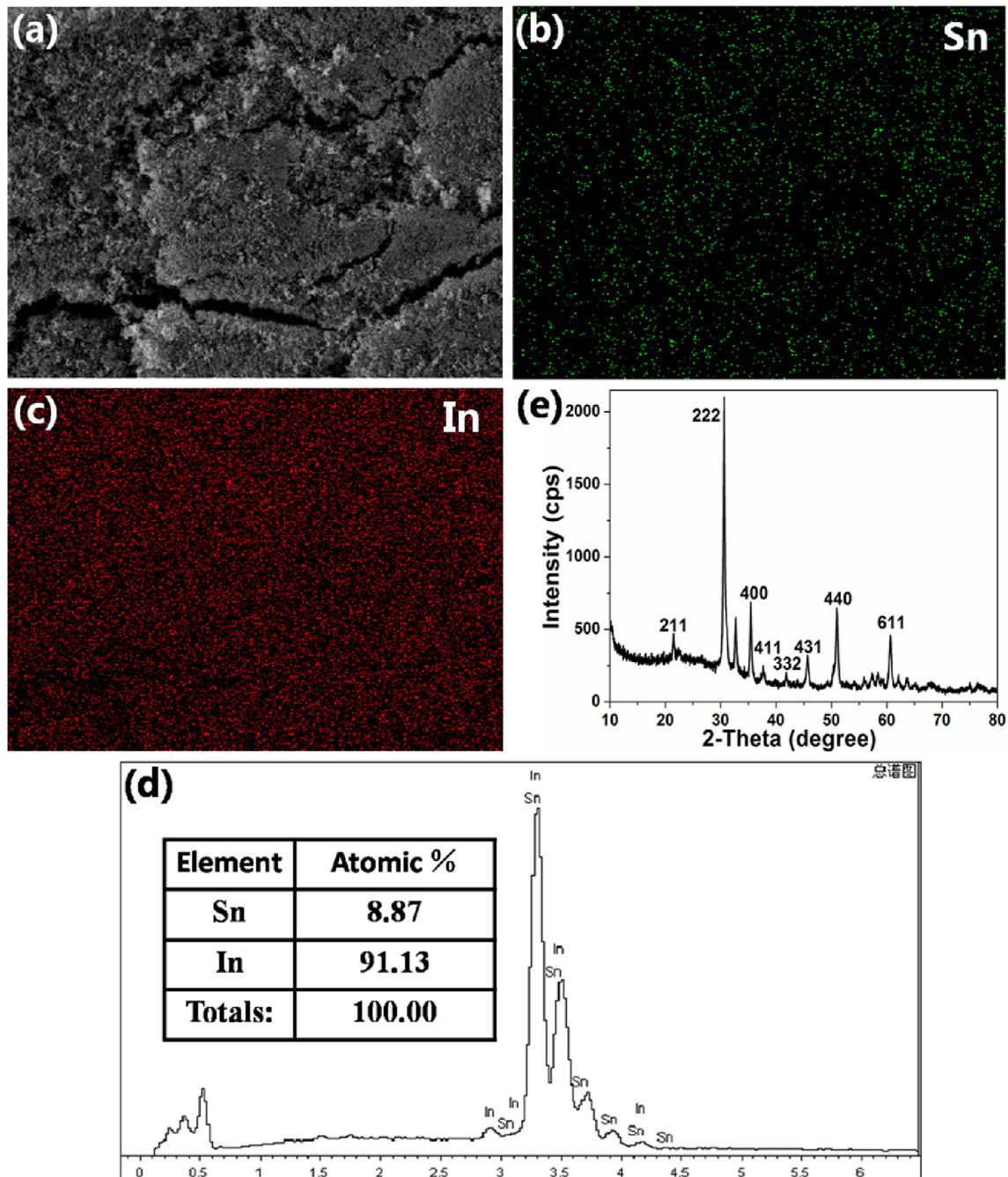


Fig. 3. (a) SEM image of the ITO nanoparticles. (b) and (c) are the element distribution of tin and indium in (a), respectively. (d) EDX data of the ITO nanoparticles. (e) The XRD of the ITO nanoparticles.

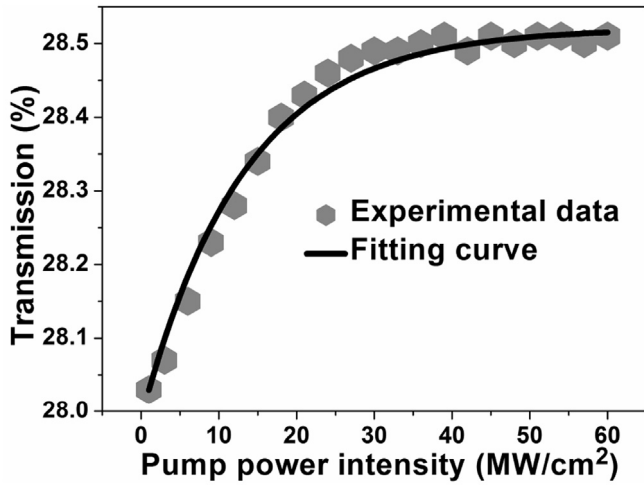


Fig. 4. Nonlinear transmission of the ITO nanoparticles as a function of pump power intensity.

U-4100) was used to measure absorption spectra of the ITO solution. X-ray Diffraction (XRD, Bruker D8) was used to characterize the crystalline quality of the ITO nanoparticles. The chemical composition of the ITO was analyzed by energy-dispersive X-ray spectroscopy (EDX, Zeiss Gemini Ultra-55).

3. Experimental results and discussions

The characterizations of the ITO are shown in Fig. 2. Fig. 2(a) shows the TEM image of the ITO nanoparticles. From this image, we can see that the size of the ITO nanoparticles is uniform. According to the statistical analysis of 100 ITO particles from the Fig. 2(a), the average size of the ITO nanoparticles is about 34.7 nm, as shown in Fig. 2(b). In order to observe more clearly, the HRTEM image of the ITO nanoparticles was obtained, as shown in Fig. 2(c). We can clearly see the lattice fringes of the ITO nanoparticles through this image, indicating the high quality of the ITO nanoparticles. In order

to obtain the absorption spectra of the ITO, we used the UV/VIS/NIR spectrophotometer to detect the ITO dispersion solution, as shown in Fig. 2(d). The ITO dispersion solution has a wide absorption bandwidth (from 1200 nm to 2000 nm) in the NIR. This is due to the nanoscale size and lower carrier density of the ITO nanoparticles. Besides, the absorption peak of the absorption spectrum is about 1642 nm. Thus, the ITO nanoparticles can serve as a promising material for photonic technologies in the NIR range.

In order to obtain more information about the structure characteristics of the ITO nanoparticles, we used EDX and XRD to analyze the obtained ITO nanoparticles, as shown in Fig. 3. As shown in Fig. 3(a), SEM image of the ITO nanoparticles was measured. The EDX technique was used to detect the element distribution of tin and indium in Fig. 3(a). Fig. 3(b) and (c) shows the distribution of tin and indium in Fig. 3(a), respectively. Fig. 3(d) shows the EDX spectroscopy from the ITO nanoparticles. The peaks corresponding to the tin and indium elements can be clearly observed from this figure. As shown in the inset of Fig. 3(d), the atom ratio of Sn: In is 8.87: 91.13. In addition, we used XRD to characterize the crystal structure of the obtained ITO nanoparticles, as shown in Fig. 3(e). The XRD pattern does not show any diffraction peaks except for ITO, which represents that we have prepared high quality ITO nanoparticles.

In order to study the nonlinear absorption properties of ITO, we used the ITO colloidal liquid to prepare a thin interface and measured it with a typical Z-scan scheme involving a balanced twin-detector measurement system. As shown in Fig. 4, the absolute transmissions of the ITO nanoparticles as the varied pump power intensity was obtained. We used a laser pulse of 480 fs with a wavelength of 1562.3 nm. The gray hexagon is the experimental data and the black line is the fitting result. We can observe that as the pump power increases, the transmittance increases rapidly and gradually saturates. The dependence of the transmittance and the pump power confirmed that the existence of saturable absorption of the ITO thin interface [27]. The relative parameters were fitted by using the following equation [28]:

$$T(I) = 1 - \Delta T \times \exp(-I/I_{sat}) - T_{ns} \tag{1}$$

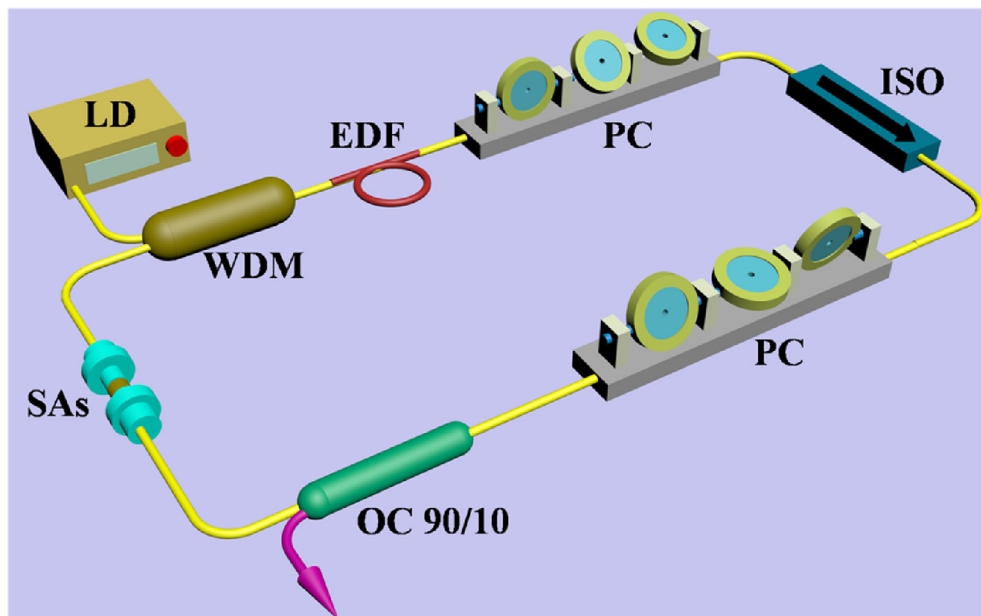


Fig. 5. Experimental configuration of the mode-locked EDF laser based on ITO SAs.

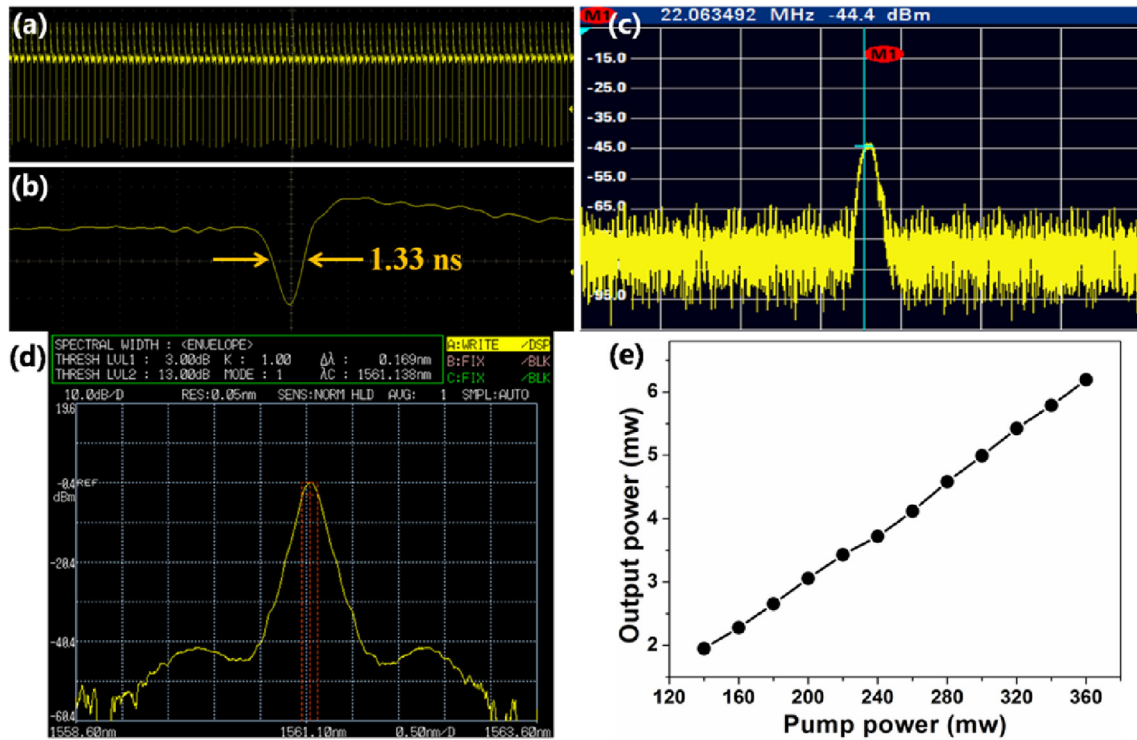


Fig. 6. Experimental results of the mode-locked EDF laser based on ITO SAs. (a) and (b) are the oscilloscope trace of dark solitons in the time scales of 400 ns/div and 2 ns/div. (c) Radio frequency (RF) spectrum of the mode-locked laser. (d) Optical spectrum of the dark solitons pulse. (e) Pump power dependence of the output power.

where T is transmission, I is input light intensity, T_{ns} is non-saturable absorbance, ΔT and I_{sat} are the modulation depth and saturation intensity, respectively. The calculated modulation depth and saturation intensity were 0.48% and 13.21 MW/cm², respectively. This result provides a good understanding of the nonlinear optical properties of ITO and also indicate that the ITO nanoparticles could be potential candidates for optical limiting applications.

Fig. 5 shows the schematic configuration of the mode-locked EDF laser incorporating the ITO-based SA. The propagation direction of the laser in the ring cavity has been marked with black arrows. A segment of erbium-doped fiber (EDF) is pumped by a 974 nm laser diode through a 980/1550 nm wavelength division multiplexing (WDM). An isolator was employed to ensure the unidirectional propagation of light in the ring cavity. By using a 90:10 optical coupler, the output from the laser cavity is extracted. The fiber flange is used to connect the output coupler and WDM. The ITO-based SA was successfully prepared by directly dropping ITO colloidal liquid into the fiber flange. The total length of the ring cavity is about 9.07 m. Besides, The total cavity group velocity dispersion is estimated to be -0.188 ps^2 at 1561.1 nm. Two polarization controllers (PC) are integrated into the ring cavity to optimize birefringence of the cavity.

By directly dropping ITO colloidal liquid into inside the mode-locked EDF laser cavity, the dark solitons pulse could be observed at a pump power of 140 mW. A series of optical spectra of the dark solitons pulses based the ITO SAs will be presented, as shown in Fig. 6. The oscilloscope trace of the dark solitons pulses train is shown in Fig. 6(a). By measuring, the pulse-to-pulse interval of the dark solitons pulses is 45.11 ns with a repetition rate of 22.17 MHz. For the fundamentally repetitive dark pulses, the pulse width was ~ 1.33 ns, as shown in Fig. 6(b). Fig. 6(c) shows the radio frequency spectrum of the dark soliton mode-locked laser with a repetition rate of 22.06 MHz. The signal-to-noise ratio is about 30.6 dB. The

optical spectrum of mode-locked pulses is centered at 1561.1 nm, as shown in Fig. 6(d). The 3 dB spectral width is 0.169 nm. The spectral resolution of the spectroscopy is 0.05 nm. The relation between the average output power and the pump power of the laser is shown in Fig. 6(e). It is noted that the dark soliton mode-locked laser output power increases linearly with the increase of pump power. As the pump power increasing from 140 to 360 mW, the output power of a single dark soliton mode-locked is increased from 1.95 to 6.19 mW, while the mode-locked operation is stable without any additional adjustment. Finally, the dark solitons cannot be obtained no matter how we adjust the pump power and PC after we remove the ITO SAs. Because the ITO SAs shows a large nonlinear refractive index [24], which can effectively induce the high nonlinear optical response.

4. Conclusions

In this paper, the production of dark soliton in EDF laser based on ITO SAs is proposed, for the first time to our best knowledge. The high quality of the ITO nanoparticles has been fabricated by using a coprecipitation method. By directly dropping ITO colloidal liquid between two fiber connectors, a novel SAs based on ITO has been obtained, which can deliver the generation of dark solitons pulse at a wavelength of 1561.1 nm with a frequency of 22.06 MHz in an EDF laser. We believe that ITO SAs device could also be used in other fiber and solid-state lasers to find important applications in the fields of ultrafast photonics in the future research.

Acknowledgements

This work is supported by National Natural Science Foundation of China (NSFC) (Grant No. 11674199, 11474187, 11405098, 61205174), Excellent Young Scholars Research Fund of Shandong Normal University, China Postdoctoral science Foundation

(2016M602177) and Shandong Provincial Natural Science Foundation (ZR2016FP01).

References

- [1] R.K. Dodd, J.C. Eilbeck, J.D. Gibbon, H.C. Morris, *Solitons and Nonlinear Wave Equations*, Academic Press, 1982.
- [2] P. Emplit, J.P. Hamaide, F. Reynaud, C. Froehly, A. Barthelemy, Picosecond steps and dark pulses through nonlinear single mode fibers, *Optic Commun.* 62 (1987) 374–379.
- [3] Y.F. Song, J. Guo, L.M. Zhao, D.Y. Shen, D.Y. Tang, 280 GHz dark soliton fiber laser, *Opt. Lett.* 39 (2014) 3484–3487.
- [4] X. Li, S. Zhang, Y. Meng, Y. Hao, Harmonic mode locking counterparts of dark pulse and dark-bright pulse pairs, *Optic Express* 21 (2013) 8409–8416.
- [5] W. Zhao, E. Bourkoff, Propagation properties of dark solitons, *Opt. Lett.* 14 (1989) 703–705.
- [6] H. Zhang, D.Y. Tang, L.M. Zhao, R.J. Knize, Vector dark domain wall solitons in a fiber ring laser, *Optic Express* 18 (2010) 4428–4433.
- [7] D. Tang, J. Guo, Y. Song, H. Zhang, L. Zhao, D. Shen, Dark soliton fiber lasers, *Optic Express* 22 (2014) 19831–19837.
- [8] G. Shao, Y. Song, J. Guo, J. Zhao, D. Shen, D. Tang, Induced dark solitary pulse in an anomalous dispersion cavity fiber laser, *Optic Express* 23 (2015) 28430–28437.
- [9] T. Sylvestre, S. Coen, P. Emplit, M. Haelterman, Self-induced modulational instability laser revisited: normal dispersion and dark-pulse train generation, *Opt. Lett.* 27 (2002) 482–484.
- [10] Y.Q. Ge, J.L. Luo, L. Li, X.X. Jin, D.Y. Tang, D.Y. Shen, S.M. Zhang, L.M. Zhao, Initial conditions for dark soliton generation in normal-dispersion fiber lasers, *Appl. Optic.* 54 (2015) 71–75.
- [11] L. Wang, Coexistence and evolution of bright pulses and dark solitons in a fiber laser, *Optic Commun.* 297 (2013) 129–132.
- [12] J.M. Ablowitz, T.P. Horikis, S.D. Nixon, D.J. Frantzeskakis, Dark solitons in mode-locked lasers, *Opt. Lett.* 36 (2011) 793–795.
- [13] Y.S. Kivshar, G. Agrawal, *Optical Solitons: from Fiber to Photonic Crystals*, Academic New York, 2003.
- [14] B.A. Malomed, A. Mostofi, P.L. Chu, Transformation of a dark soliton into a bright pulse, *J. Opt. Soc. Am. B* 17 (2000) 507–513.
- [15] X. Wang, P. Zhou, X. Wang, H. Xiao, Z. Liu, 2 μm bright–dark pulses in Tm-doped fiber ring laser with net anomalous dispersion, *APEX* 7 (2014), 022704.
- [16] Y.S. Kivshar, P. Emplit, J.P. Hamaide, M. Haelterman, Gordon–Haus effect on dark solitons, *Opt. Lett.* 19 (1994) 19–21.
- [17] H. Zhang, D.Y. Tang, L.M. Zhao, X. Wu, Dark pulse emission of a fiber laser, *Phys. Rev. A* 80 (2009), 045803.
- [18] W. Liu, L. Pang, H. Han, Z. Shen, M. Lei, H. Teng, Z. Wei, Dark solitons in WS₂ erbium-doped fiber lasers, *Photon. Res.* 4 (2016) 111–114.
- [19] W. Liu, L. Pang, H. Han, W. Tian, H. Chen, M. Lei, P. Yan, Z. Wei, Generation of dark solitons in erbium-doped fiber lasers based Sb₂Te₃ saturable absorbers, *Optic Express* 23 (2015) 26023–26031.
- [20] J.Q. Zhao, Y.G. Wang, P.G. Yan, S.C. Ruan, G.L. Zhang, H.Q. Li, Y.H. Tsang, An L-band graphene-oxide mode-locked fiber laser delivering bright and dark pulses, *Laser Phys.* 23 (2013) 075105.
- [21] Q. Guo, Y. Yao, Z.C. Luo, Z. Qin, G. Xie, M. Liu, J. Kang, S. Zhang, G. Bi, X. Liu, J. Qiu, Universal near-infrared and mid-infrared optical modulation for ultrafast pulse generation enabled by colloidal plasmonic semiconductor nanocrystals, *ACS Nano* 10 (2016) 9463–9469.
- [22] X. Liu, Q. Guo, J. Qiu, Emerging low-dimensional materials for nonlinear optics and ultrafast photonics, *Adv. Mater.* 29 (2017) 827–846.
- [23] G.V. Naik, V.M. Shalaev, A. Boltasseva, Alternative plasmonic materials: beyond gold and silver, *Adv. Mater.* 25 (2013) 3264–3294.
- [24] M.Z. Alam, I. De Leon, R.W. Boyd, Large optical nonlinearity of indium tin oxide in its epsilon-near-zero region, *Science* 352 (2016) 795–797.
- [25] G.V. Naik, V.M. Shalaev, A. Boltasseva, Alternative plasmonic materials: beyond gold and silver, *Adv. Mater.* 25 (2013) 3264–3294.
- [26] M. Kanehara, H. Koike, T. Yoshinaga, T. Teranishi, Indium tin oxide nanoparticles with compositionally tunable surface plasmon resonance frequencies in the near-IR region, *J. Am. Chem. Soc.* 131 (2009) 17736–17737.
- [27] I.V. Kityk, Q. Liu, Z. Sun, J. Fang, Low-temperature anomalies of two-proton absorption in In₂O₃ nanocrystals incorporated into PMMA matrixes, *J. Phys. Chem. B* 110 (2006) 8219–8222.
- [28] J. Li, H. Luo, B. Zhai, R. Lu, Z. Guo, H. Zhang, Y. Liu, Black phosphorus: a two-dimension saturable absorption material for mid-infrared Q-switched and mode-locked fiber lasers, *Sci. Rep.* 6 (2016) 30361.